HAL open science

A 6-components mechanistic model of cutting forces and moments in milling

Maël Jeulin, Olivier Cahuc, Philippe Darnis, Raynald Laheurte

To cite this version:

Maël Jeulin, Olivier Cahuc, Philippe Darnis, Raynald Laheurte. A 6-components mechanistic model of cutting forces and moments in milling. Forces in Mechanics, 2022. hal-03971908

HAL Id: hal-03971908

https://hal.science/hal-03971908v1

Submitted on 3 Feb 2023

HAL is a multi-disciplinary open access archive for the deposit and dissemination of scientific research documents, whether they are published or not. The documents may come from teaching and research institutions in France or abroad, or from public or private research centers.

L'archive ouverte pluridisciplinaire **HAL**, est destinée au dépôt et à la diffusion de documents scientifiques de niveau recherche, publiés ou non, émanant des établissements d'enseignement et de recherche français ou étrangers, des laboratoires publics ou privés.

Distributed under a Creative Commons Attribution 4.0 International License

Forces in Mechanics 9 (2022) 100130

Contents lists available at ScienceDirect

Forces in Mechanics

journal homepage: www.sciencedirect.com/journal/forces-in-mechanics

A 6-components mechanistic model of cutting forces and moments in milling

Maël Jeulin *, Olivier Cahuc, Philippe Darnis, Raynald Laheurte

University Bordeaux, I2M UMR 5295, 351 cours de la Liberation, Talence F-33400, France

ARTICLE INFO

Keywords:
3-dimensional milling
Energy balance
Cutting moment
Cutting model
3-dimensional chip section

ABSTRACT

Most of the cutting models developed in the literature attest only to the presence of cutting forces in the balance of mechanical energy resulting from cutting. However, several studies [1–4] have highlighted the presence of cutting moments during machining, and particularly for milling. From a theoretical point of view, a complete energy balance must integrate all the components of the mechanical actions (forces and moments). The predictive model of this study proposes to characterize the evolution of the moments in the cutting zone for milling. The objective is to determine a model similar to the cutting forces which expresses a relationship with the chip section define by the Kc coefficient but by integrating the specific behavior of the moments. This work gives perspectives from an energetic point of view for which the part of moments in the energy balance could be substantial for specific configurations as small-radius tools or high-speed milling.

Introduction

Machining processes modelling constitute a substantial amount of work in the mechanical engineering literature. Products quality sustainability, new manufacturing processes or even digital manufacturing are the main issues of this field. In order to improve the sustainability of machining processes, this paper focus on a mechanistic model of the cutting in milling which allow a complete and accurate energy evaluation.

Correctly predicting the mechanical energy makes it possible to anticipate manufacturing costs and even its environmental impact. To predict the consumed energy models in the literature [1–4] are based on the mechanical cutting models. For many authors [5–8] cutting models were developed considering exclusively cutting forces for the mechanical actions as source of the consumed energy.

For these papers [5–8] the geometrical and kinematic parameters of orthogonal cutting have been considered. For other authors [9–11] the influence of material parameters for example (hardness, thermal conductivity, mechanical strength) have been carried out.

To respect theory, the consumed energy is based on all the mechanical actions. Mechanical models have to consider the 3 forces and 3 moments components especially in machining as hard cutting processes or high-speed machining [12]. For these configurations, the contribution of the cutting moments constitutes an important part of the consumed energy in machining and can be as high as 40% for conventional machining and up to 80% for high-speed machining [12–14].

Authors [15,16] have developed models of the cutting moments for milling process and turning with vibrations. This works expressed the linear relations between moments and the chip section. The presented article aims to generalize the definition of cutting moments.

This paper describes an experimental model integrating the cutting moments for a specific configuration and gives tools to predict these coefficients in 3D cutting. The proposed results are the first part of a more complete experimental model. In the first section, the 3D cutting model considered is defined. Then, the experimental protocol and the material used are described. Finally, the last paragraph is devoted to the results and their analysis, to propose a mechanistic model of cutting moments.

1. Milling cutting model

1.1. State of the art

The 3D geometrical parameters of the tooth orientation for a milling operation [1,3] are defined in Fig. 1 with respect to the tooth's rotational reference ($\vec{e_r}$, $\vec{e_\theta}$, $\vec{z_0}$), as well as the description of the orthogonal cutting ($\lambda_s = 0°$, $\kappa_r = 90°$, any γ_0). Mechanical cutting models are most commonly based on the chip section [5–8]. This section is described by the cutting plan $\mathscr{R}_{cp}$ directly in contact between the workpiece and the

* Corresponding author.
E-mail address: mael.jeulin@u-bordeaux.fr (M. Jeulin).

https://doi.org/10.1016/j.finmec.2022.100130
Received 30 July 2022; Received in revised form 28 September 2022; Accepted 6 October 2022
Available online 7 October 2022
2666-3597/© 2022 The Author(s). Published by Elsevier Ltd. This is an open access article under the CC BY license (http://creativecommons.org/licenses/by/4.0/).

Nomenclature

t	tool
wp	workpiece
V_c	cutting speed (m/min)
V_f	feed velocity (m/min)
f	feed rate (mm/tr)
a_p	depth of cut (mm)
κ_r	tool cutting edge angle (°)
γ_0	rake angle (°)
λ_s	cutting edge inclination (°)
C_c	tool centre position
C_e	cutting edge position
$\mathscr{R}_0$ (O, $\overrightarrow{x_0}$, $\overrightarrow{y_0}$, $\overrightarrow{z_0}$)	fixed reference of the sensor applied to the measure origin O
$\mathscr{R}_t$ (C_e, $\overrightarrow{e_r}$, $\overrightarrow{e_\theta}$, $\overrightarrow{z_0}$)	local reference mark of the lathe applied to the cutting edge position C_e
$\mathscr{R}_{cp}$ (P, $\overrightarrow{e_{r_{cp}}}$, $\overrightarrow{e_{\theta_{cp}}}$, $\overrightarrow{z_{cp}}$)	local cutting plane reference applied to the application point of the cutting P
θ	angular position of the cutting edge (°)
$\overrightarrow{\omega}_{t/wp}$ ($\overrightarrow{\omega}$)	angular speed field of the tool relative to the workpiece
$\overrightarrow{V}_{P,t/wp}$ ($\overrightarrow{V}_P$)	velocity field of the tool relative to the workpiece at point P
$\overrightarrow{\mathscr{F}}_{wp\to t}$	force field of the workpiece on the tool
$\overrightarrow{\mathscr{M}}_{P,wp\to t}$	moment field of the workpiece on the tool at point P
Y_c	y_0-axis coordinate of the tool center (mm)
$S_{chip\ 3D}$	chip section (mm^2)
Δe_r	instantaneous radial feed rate (mm)
Δf	instantaneous axial feed rate (mm)
$C_{*,i}(\theta_j)$	discretized position in round of cut i, at discretized angular position θ_j
ω_z	tool angular speed (rad/s)
K_c	specific cutting pressure (N/mm^2)
K_m	specific cutting moment density $(N.m/mm^2)$
F, M	designated force and moment components

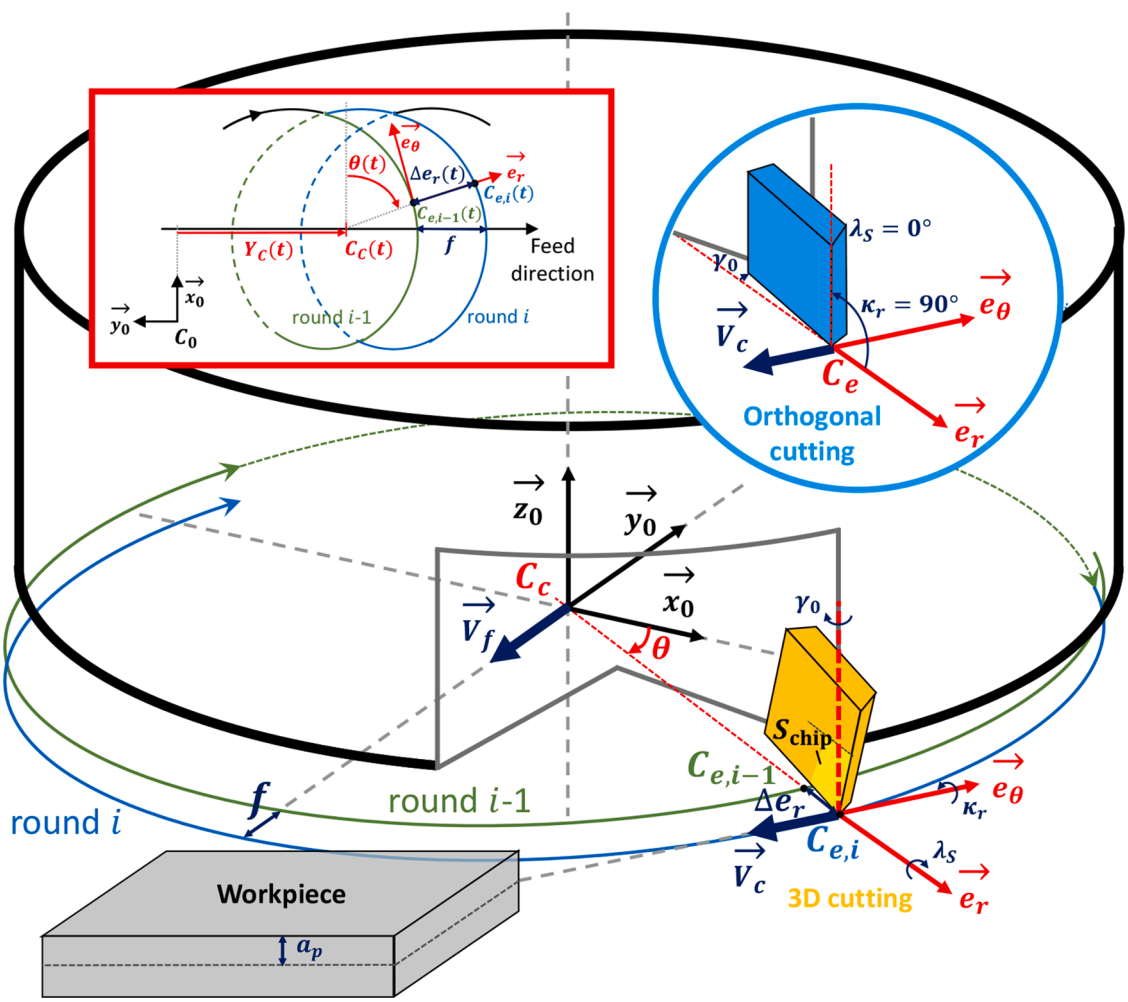

Fig. 1. Definition and configuration of the cutting.

tool, following the trochoidal trajectory of the tool tip (Fig. 1). Quantities of tests in the literature have therefore been carried out in orthogonal cutting to establish simple and usable cutting models associated with cutting forces. The first model that considers linear cutting forces according to the chip section was introduced by Martellotti [17], with cutting pressure coefficient K_c workpiece material-specific:

$$\mathscr{F}_{\mathrm{t}\rightarrow\mathrm{wp}} = K_c \times S_{\mathrm{chip\ 3D}} \tag{1}$$

The coefficient K_c is dependent on the tool feed rate, determined by the Victor-Kienzle equation [18], where K_{c1} and m_c are material dependent parameters and f_0 the feed rate scaling parameter:

$$K_c = K_{c1}\cdot(f/f_0)^{-m_c} \tag{2}$$

Such a model is sufficient to correctly predict the cutting forces and will be verified experimentally in Section 3.1. The objective of the paper is to verify whether such kind of models are also applicable to cutting moments. Basic orthogonal cutting models, that have only developed the importance of cutting forces linearly dependent on the chip section, present significant errors in their modelled energy consumption [12,13]. This is why the development of cutting moments theory was a major step towards completing the cutting energy balance. Several studies have therefore identified the main sources of cutting moment creation as follows:

- Pure torques related to intra-grain spin at the microstructural scale of the material, caused by high cutting stresses [12,19,20].
- Torques induced by the 3D geometric and kinematic cutting phenomenology [21,22].
- Frictional moments generated by intense tribological phenomena at the tool/workpiece/chip interface with specific friction conditions (high pressure and temperature, strain hardening, variable chip section, etc.), studied mainly in the literature on cutting forces [23], but also applicable to cutting moments.

1.2. Model assumptions

Studies have attempted to model cutting moments, such as Albert et al. [15] who started to model the cutting moment phenomenology with orthogonal cutting tests in milling, or Cahuc et al. [16] with turning tests. For the proposed model, the point of expression where the modelling is most relevant should be defined. The value of the cutting moments is different depending on the application point, so it is essential to establish a significant point P to express the cutting moments. Albert et al. [15] proposed to model the cutting moments in the middle of the main cutting edge. The theoretical application point of the cutting P should be at the barycentre of the tool force density on the workpiece. This point is complex to determine experimentally because the measurement of forces and moments is the force vector and not the measurement of the cutting force density. The application point P is assumed to be located in the cutting zone, as this is the most physically significant area with the cutting force density concentrated on it. The position of point P will be determined experimentally and compared to that proposed by Albert et al. [15] in Section 3.2.

The theoretical application point P of the cutting is a secondary element for the energy balance and is only a calculation point for the mechanical power. The mechanical power (which represents the consumed machining power [13]) does not depend on the application point nor on the expression reference of the mechanical and kinematic components. In the context of machining, the hypothesis of undeformable solids is used because the forces and moments components of the energy balance are measured and global. The internal mechanical power developed by machining, calculated at the point P, is then described [12–14]:

$$\mathscr{P}_{\mathrm{t}\leftrightarrow\mathrm{wp}} = \overrightarrow{\mathscr{F}}_{\mathrm{wp}\rightarrow\mathrm{t}}\cdot\overrightarrow{V}_{P,\mathrm{t/wp}} + \overrightarrow{\mathscr{M}}_{P,\mathrm{wp}\rightarrow\mathrm{t}}\cdot\overrightarrow{\omega}_{\mathrm{t/wp}} \tag{3}$$

The type of model chosen for cutting forces [17] has been described previously, it is then necessary to define the one associated with cutting moments. The objective is to achieve a mechanistic model in order to completely describe the power consumed by the machining, and not a phenomenological model which would present shortcomings in the identification of complete cutting moments. This is the case of Yousfi et al. [22] who succeed in identifying only 10% of real cutting moments with their phenomenological model. A linear model as a function of the chip section is therefore proposed as the model associated with the cutting moments in conventional milling, with the coefficient K_m [N.m.mm^{-2}], in order to propose a model similar to that of the cutting forces [17]. This coefficient represents the specific cutting moment density by equivalence to the specific cutting pressure K_c. The complex phenomenon of hysteresis observed for climb milling (observed in Figs. 7 and 8), which also shows a certain linearity in relation to the chip section, remains to be investigated. The framework of this model is justified in Section 3.3, which presents the independence of the depth of cut on the K_m coefficient, and demonstrates the complexity of the climb milling part. In addition, the modelings of the paper are carried out on the moments that influence the energy balance of the cutting, therefore only those developed along the z-axis. The model adopted will be discussed in Section 3.3 and is therefore of the following form:

$$\overrightarrow{\mathscr{M}}_{P,\mathrm{wp}\rightarrow\mathrm{t}}\cdot\overrightarrow{z} = K_m \times S_{\mathrm{chip\ 3D}} \tag{4}$$

Numerous orthogonal cutting tests carried out by Albert et al. [15] have enabled initial interpretations and models of cutting moments. An interesting result is the influence of the orthogonal parameters V_c, f, a_p on the preponderance of cutting moments. Albert [24] demonstrated with the results of his design of experiments, an independence of the cutting parameters (negligible interaction between the parameters) on the value of cutting moments. This assumption of cutting parameter independence is verified experimentally in this paper. As the cutting parameters are the predominant factors in the evolution of the cutting forces [3,5] and moments [12,13,15], the parameter K_m of the cutting moments model in conventional milling are considered to be dependent only on these. A preliminary cutting parameter-based modelling will then be proposed in Section 3.3.

In the energy balance, there is the mechanical aspect highlighted by the modelling proposed of cutting forces and moments, however the kinematic fields must also be defined. As each machine position $\overrightarrow{Pos_P}(X_P, Y_P, Z_P)$ at point P is discretized at regular time intervals Δt, the instantaneous local speed $\overrightarrow{V_P}$ is defined as follows:

$$\overrightarrow{V_P} = \frac{\overrightarrow{\Delta Pos_P}}{\Delta t} \tag{5}$$

This velocity can be applied to the local basis ($C_{e,i}$, $\overrightarrow{e_r}$, $\overrightarrow{e_\theta}$, $\overrightarrow{z_0}$) turned at the discretized θ_j angle:

$$\begin{cases} V_{C_{e,i},e_r} & \left(\Delta X_{C_{e,i}}\cos\theta_j + \Delta Y_{C_{e,i}}\sin\theta_j\right)/\Delta t \\ V_{C_{e,i},e_\theta} & \left(\Delta Y_{C_{e,i}}\cos\theta_j - \Delta X_{C_{e,i}}\sin\theta_j\right)/\Delta t \\ V_{C_{e,i},z_0} & \Delta Z_{C_{e,i}}/\Delta t \end{cases}$$

Intrinsic variations of the (X_{C_e}, Y_{C_e}, Z_{C_e}) components from the nominal trochoidal path may correspond to the deceleration of the tool demonstrated by the variation of the instantaneous axial feed rate Δf. The machining configuration is assumed to be stabilised, i.e. the absence of vibration is considered, which is equivalent to $\Delta Z_{C_{e,i}} = 0$.

The tool rotational speed $\omega_{z,j}$ is defined such that it accounts for the deceleration of the tool during the cutting process:

$$\omega_{z,j} = \Delta\theta_{j,j-1}/\Delta t \tag{6}$$

2. Experimental approach

An experimental set-up was carried out to develop the experimental

mechanistic model of the cutting phenomenon wanted. In order to fully characterise the cutting forces and moments during a cutting pass, a groove milling operation (100% radial depth of cut) is chosen as the test one. The cutting forces as well as the cutting moments will be acquired during the cutting process, treated and then analysed in Section 3.

2.1. Material used

To perform the milling tests, a 3-axis **Rosilio** C850 machine-tool was used (Table 1). The experimental setup is shown in Fig. 2. It consists of a **Kistler** 9129AA 6-component high dynamic force dynamometer (Table 2) directly fixed on the machine-tool table. Subsequently, this stage supports the AISI 4142 (42CrMo4) alloy steel samples chosen to characterise the tests for which the composition is described Table 3.

To recover the data from the dynamometer and the machine-tool, a post-processing software **DeweSoft** is used. It allows the recovery of the force and moment components developed during machining as well as the machine positions. The acquisition frequency is set at 50 kHz to characterise the cutting process of a few hundredths of a second, varying according to the imposed cutting speed.

The tool used for the cutting tests is an **ISCAR** HOF D040-04-22-R06 milling cutter having a single tooth with an **ISCAR** OEMW 060405-AETN IC808 octagonal carbide insert with Aluminium-Titanium-Nitride (AlTiN) coating (Fig. 2) and measured orientation geometry parameters $\gamma_0 = 0°$, $\kappa_r = 38°$, $\lambda_s = 15°$.

In order to get usable results, filtering of the data is necessary to

Table 1
Characteristics of the **Rosilio** C850.

Max spindle power (*kW*)	Max spindle speed (*rpm*)	Axis strokes (*mm*)	Feed rates (*m/min*)	Digital control
20	15000	X: 800 Y: 510 Z: 610	X: 20 Y: 20 Z: 24	Heidenhain ITNC 530

Table 2
Characteristics of the **Kistler** dynamometer.

Number of sensors	Max of permitted measuring range of forces (*kN*)	Max of permitted measuring range of moments (*N.m*)
4	-10 ... 10	-500 ... 500

Table 3
Chemical composition of the AISI 4142 (42CrMo4) alloy steel.

(%)	C	Si	Mn	P	S	Cr	Mo
from	0.38	-	0.60	-	-	0.90	0.15
to	0.45	0.40	0.90	0.25	0.35	1.20	0.30

Fig. 2. Experimental setup for milling tests.

Table 4
Milling design of experiments.

N° tests	V_c (m/min)	f (mm/tooth)	a_p (mm)
1 (RT)	240	0.1	1
2	120	0.1	1
3	240	0.2	1
4	120	0.2	1
5	240	0.1	2
6	120	0.1	2
7	240	0.2	2
8	120	0.2	2

eliminate the noise caused by the very high dynamics of the measurement system. As the noise appears at high frequency, a low-pass filter is used for each test over several dozen rounds to recover only the frequency around the number of rounds of cut per second, which is at a rather low frequency as the cutting speeds are reasonable. This frequency corresponds to the amplitude of the periodic phenomena of the cutting, thus the relevant cutting forces and moments.

2.2. Experimental protocol

The primary objective of the tests is to characterise the cutting moments in the cutting zone and the secondary one is to verify the influence of the cutting parameters V_c, f, a_p on the value of these cutting moments. For this purpose, a reference test (RT) characteristic of the machining with $V_c = 240\,\text{m/min}$, $f = 0.1\,\text{mm/tooth}$, $a_p = 1\,\text{mm}$ is carried out, followed by a design of experiments with the variation of the 3 parameters on 2 levels compared to the reference test. The design of experiments carried out is described in Table 4.

3. Results of cutting moments identification

3.1. Verification of the linear model of cutting forces

The first step is to verify whether a linear model as a function of the chip section can correspond to the cutting force profile. Fig. 3 shows a linear model, as a function of the chip section $S_{\text{chip 3D}}$, fitting the cutting forces along the axis $\vec{e_\theta}$ for instance. These results satisfy the cutting force models proposed in the literature [17], and the energy impact of these cutting forces compared to that of the cutting moments will be studied in Section 3.3. The 95% prediction interval shown in Fig. 3 describes the confidence interval for which 95% of the fitted data are between the 2 error bars.

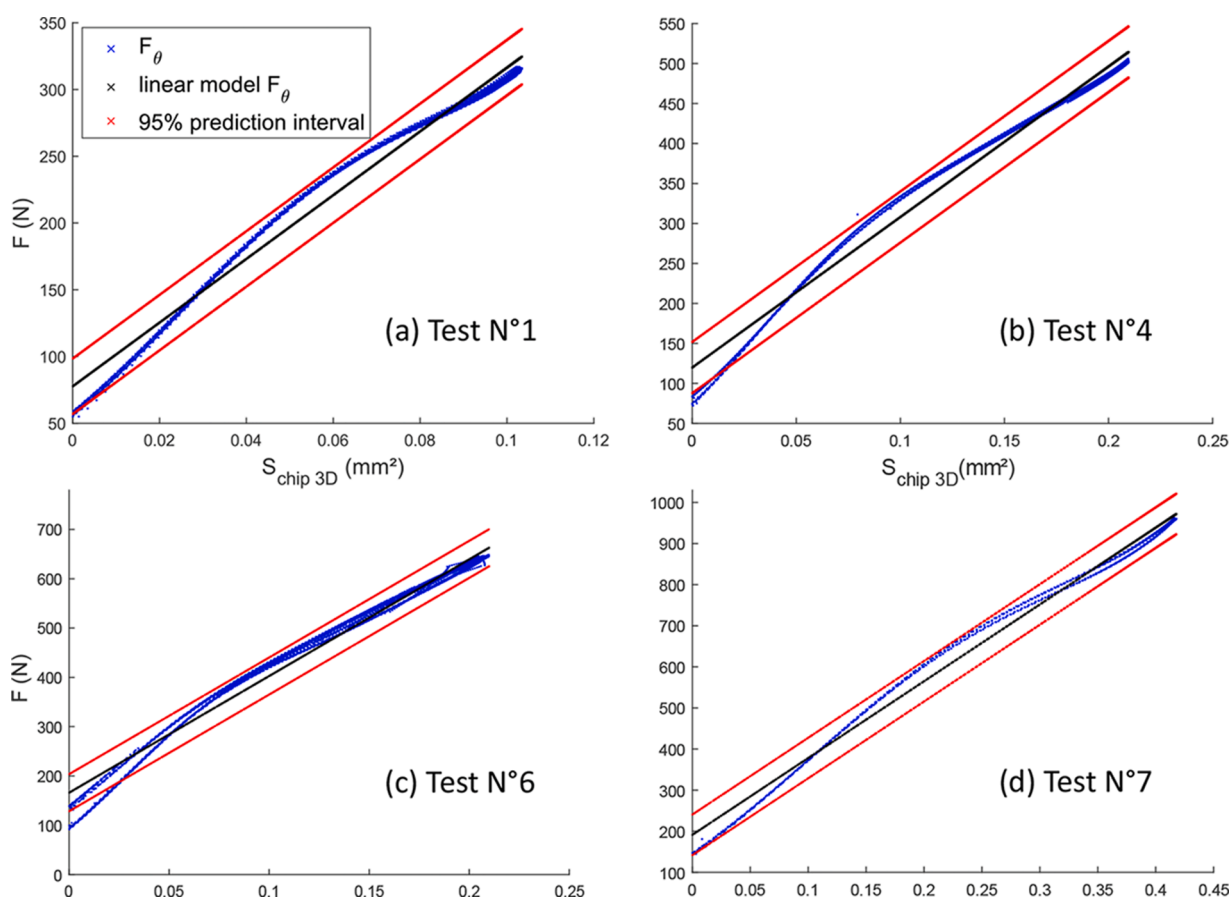

Fig. 3. Linear model of cutting forces by $S_{\text{chip 3D}}$.

3.2. Experimental results and verifications of the cutting moments

The resulting pure moments applied to the cutting points P in the cutting plane reference frame $\mathscr{R}_{cp}$ are represented by the angular position of the cutting edge θ in Fig. 4. The existence of the 3D moments highlighted in Fig. 4 is indicative of the complexity of the cutting phenomena.

To validate the presence of pure cutting moments, which are those that directly influence the energy consumption of machining, it is sufficient that the proportion of power related to moments in the energy balance is non-null. Furthermore, the central axis theory can then be used to calculate the value of these pure cutting moments according to the angular position of the cutting edge θ (Fig. 5), as suggested by Albert [24]. The presence of non-negligible moments indicates the relevance of the observed phenomenon and confirm the veracity of previous work on cutting moments [12,13,15,16].

The positioning of the application point of the cutting P can be estimated experimentally from a minimisation criterion of the cutting moments at the tool/workpiece interface, as the experimentally determined central axis is remote from the cutting zone and therefore has no physical significance. The points resulting from this criterion are those which minimise the contribution of the forces to the amplitude of the cutting moments in the cutting zone. The positions of the points P in the cutting plane reference $\mathscr{R}_{cp}$ for each discretized angular position θ are represented in Fig. 6. The points P are located in the index position where the associated minimisation criterion of the cutting moments $\min\| \overrightarrow{\mathscr{M}_{\text{mesh}}} \|$ is verified.

The position of the points P is close to the principal cutting edge, where the density of the cutting forces is the highest (separation edge of the material), and also on the average line of the chip section, which reflects the homogeneity of the cutting pressures along the direction of the cutting edge $\overrightarrow{z_{cp}}$. This is why the points P at the principal cutting edge and on the average line of the chip section were accepted to model the cutting moments (P characteristic point of the model on the Fig. 6). The associated leverage for the positioning error of the chosen point P related to the theoretical points P is minor and it is more convenient to have a fixed application point in the cutting zone than a distribution of points P. This point fits perfectly with what was proposed as a modelling point by Albert et al. [15] in orthogonal cutting.

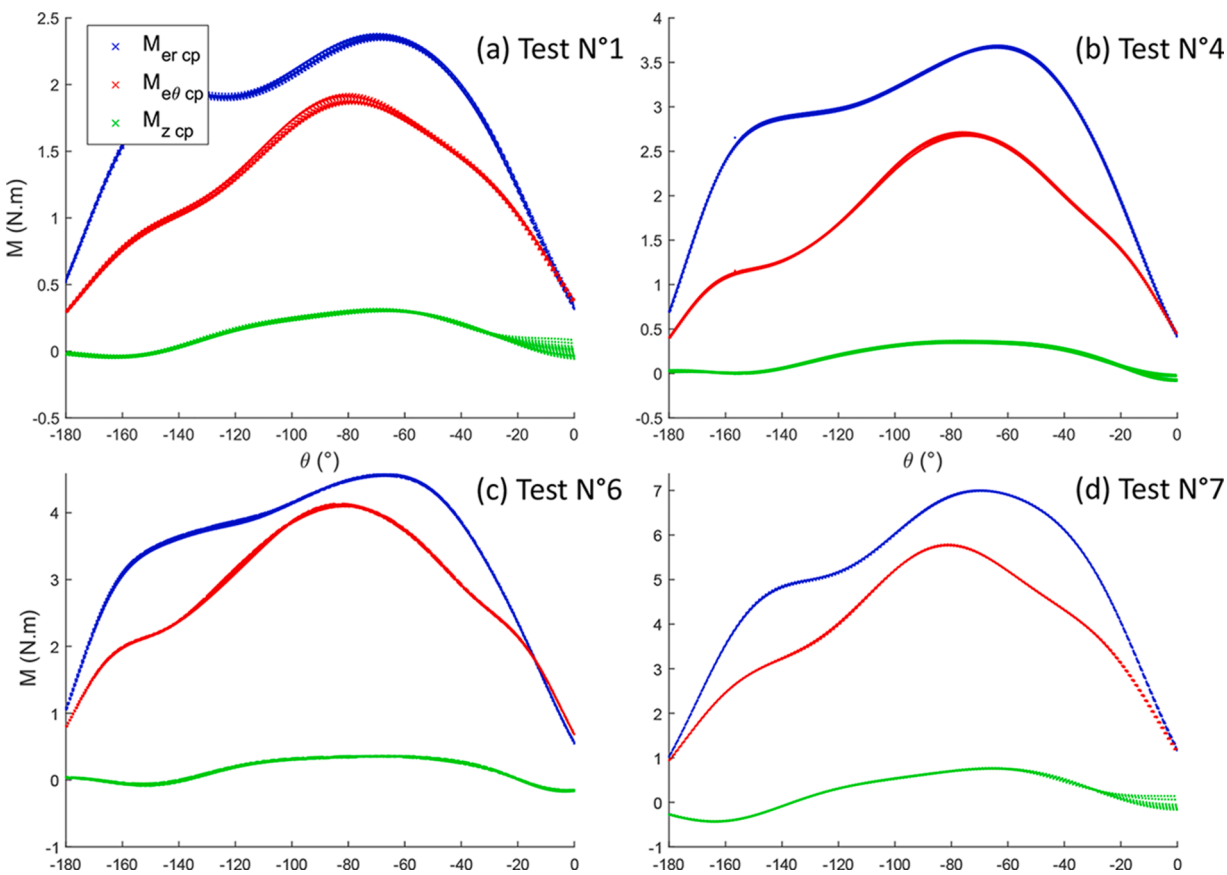

Fig. 4. 3D cutting moments at points P in $\mathscr{R}_{cp}$.

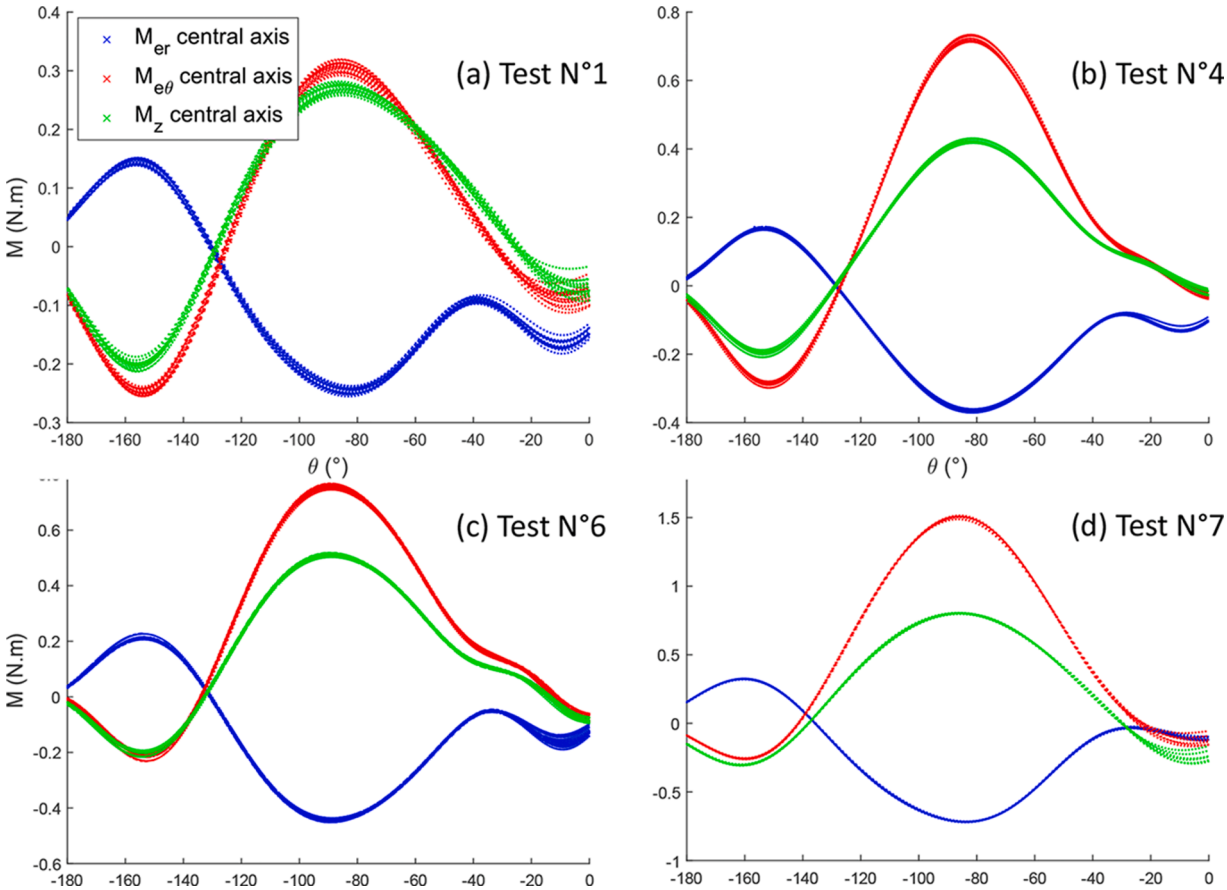

Fig. 5. Pure cutting moments expressed at the central axis in $\mathscr{R}_t$.

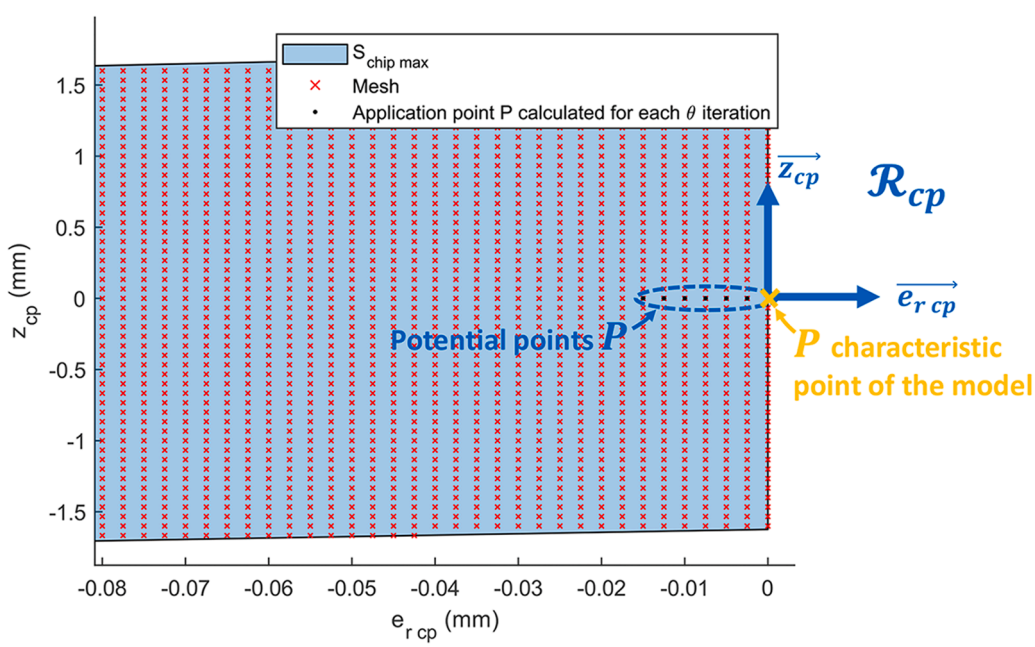

Fig. 6. Positioning of the application points of the cutting P in $\mathscr{R}_{cp}$.

3.3. Identification of specific cutting moment model

The test that will illustrate the modelling is the reference one with parameters $Vc = 240\,\mathrm{m/min}$, $f = 0.1\,\mathrm{mm}$, $ap = 1\,\mathrm{mm}$. In a first approach, a linear model only for the part corresponding to the conventional cutting mode of the tool is proposed, as a function of chip section (Fig. 7). The chosen model allows for a relatively low Root Mean Square Error (RMSE) of $0.016\,N.m$ while still having the simplicity and the physical meaning of being a specific cutting moment density coefficient. The hypothesis of the linear model in conventional milling presented can be extended to all permissible depths of cut of the insert, some of which are shown in Fig. 8.

The cutting energy balance is described in Fig. 9 with and without considering cutting moments in addition to cutting forces. It highlights the impact of the cutting moments in the energy balance, as predicted by previous studies [12,13,15,16], with a maximum absolute error up to

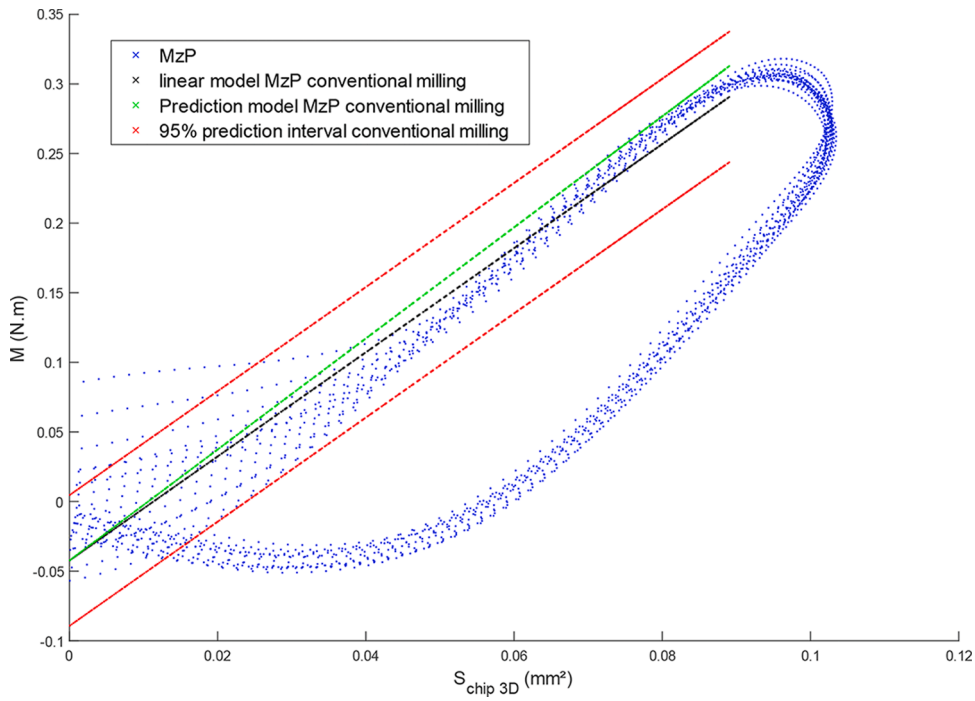

Fig. 7. Linear model of cutting moments at points P by $S_{\text{chip 3D}}$ in conventional milling.

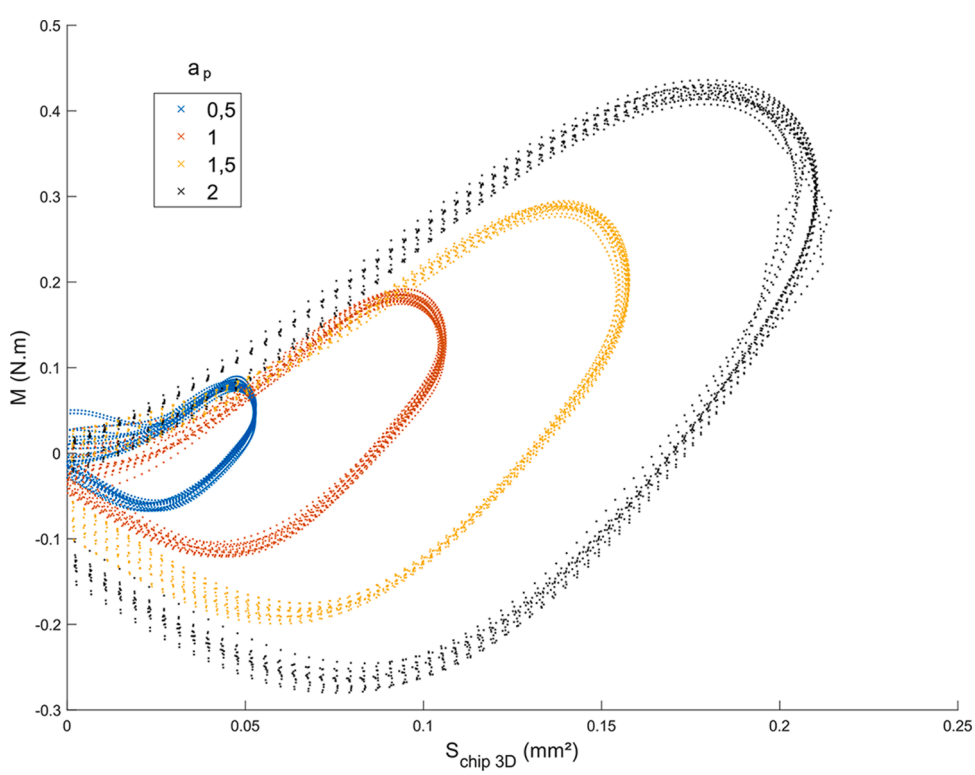

Fig. 8. Validity range of the linear model in conventional milling.

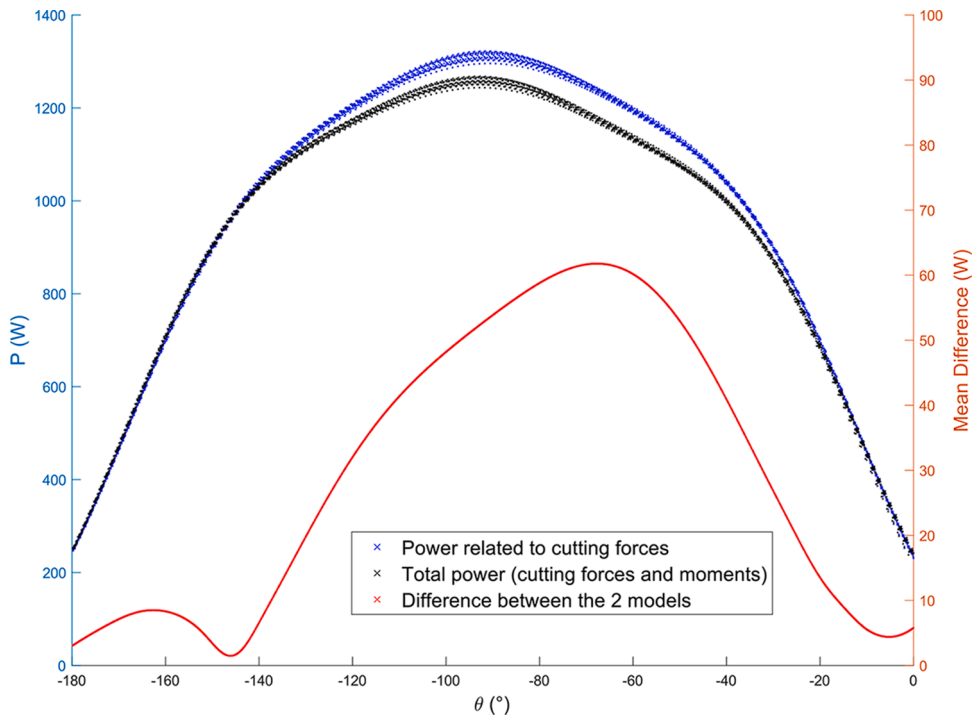

Fig. 9. Power consumed during milling.

60 W without considering the cutting moments, for the reference test.

Considering the experimental results, conclusions can be drawn on the influence of the cutting parameters V_c, f, a_p on the value of the model coefficient K_m. The parameter independence results demonstrated by Albert [24] and Victor-Kienzle [18] can be verified with these tests and even the non-influence of the parameters V_c and a_p on the value of K_m. Considering the validity zone of the cutting parameters, the following model is proposed to predict cutting moments in milling:

$$K_m = 1.27 \cdot (f)^{-0.5} \tag{7}$$

The linear plan to verify the validity of the model proposed is described in Fig. 10. The vertical error bars represent the RMSE of the K_m determination that can be fitted to the experimental results. The horizontal error bars, on the other hand, graphically describe the accuracy of the multilinear model based on the RMSE of the K_m prediction which is 0.0764 N.m.mm^{-2}, but which has non-negligible errors for some tests such as number 6. To provide an overview of the accuracy of the model, Fig. 7 highlights the efficiency of the predicted moments for the reference test.

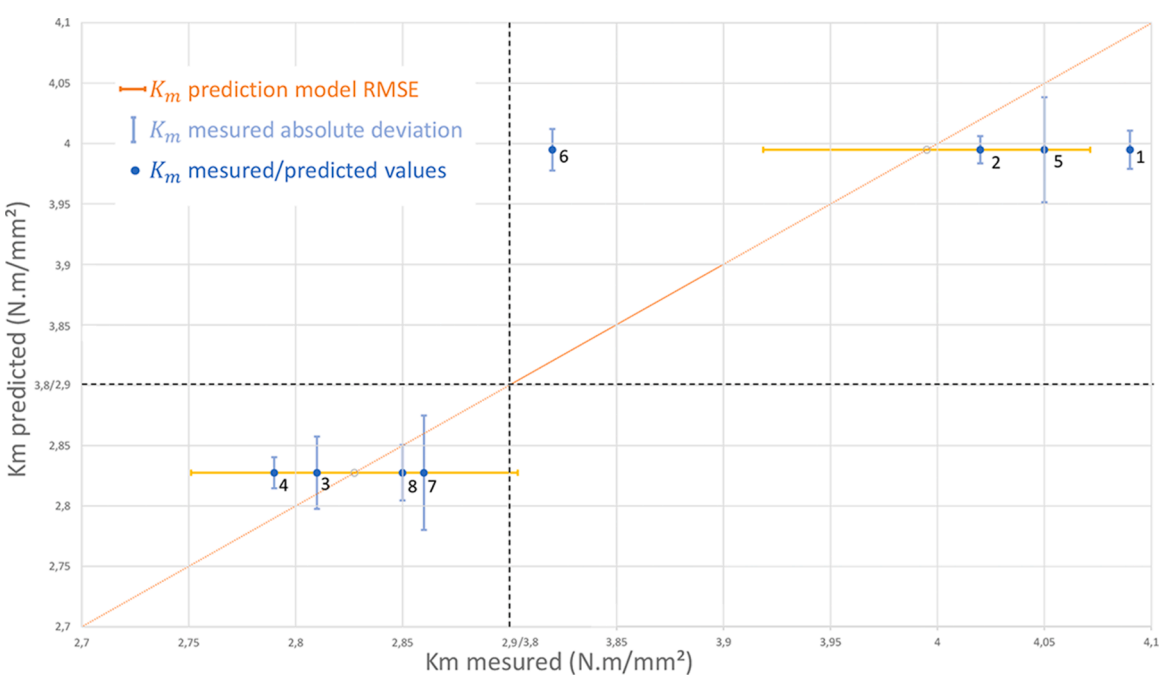

Fig. 10. Feedrate-based model of K_m.

4. Conclusion

The results proposed in this paper highlight a complex phenomenon of cutting forces and moments during milling. The moments in the cutting zone have a non-negligible impact on the power consumed by the process. Up to 5% error between the power considering only the cutting forces and the total power can be observed through the tests of this paper. The better the cutting moment phenomenon is understood, the more accurate the prediction of power consumption during machining.

The simple mechanistic model proposed to characterise these moments in the cutting zone is limited only to the conventional milling part. It shows a relatively large error but which is still acceptable for an experimental model. The proposed model is the first to fit analytically the cutting moments in relation to the chip section for a 3D-milling operation and can be enriched to reduce the associated error, particularly with others machining configurations.

The future work to be carried out to refine the model and better characterise the phenomena associated with cutting moments consists of:

- Realization of different experiments to refine and enrich the proposed mechanistic model, tests for different machining configurations (tools, materials, cutting conditions) are planned to provide a more complete database of K_m coefficients, especially tests with several feed rates to verify that the model follows a Victor-Kienzle type equation [18]
- Modelling and characterisation of the hysteresis phenomenon in climb milling
- Work on the repercussions of cutting moments on the mechanical properties of the workpiece, such as roughness, surface, hardness, residual stresses, etc.

Declaration of Competing Interest

The authors declare that they have no known competing financial interests or personal relationships that could have appeared to influence the work reported in this paper.

References

[1] E. Usui, A. Hirota, M. Masuko, Analytical prediction of three dimensional cutting process-part 1: basic cutting model and energy approach, J. Eng. Ind. 100 (2) (1978) 222–228, https://doi.org/10.1115/1.3439413.

[2] I. Lazoglu, S.Y. Liang, Modeling of ball-end milling forces with cutter axis inclination, J. Manuf. Sci. Eng. 122 (1) (1999) 3–11, https://doi.org/10.1115/1.538885.

[3] Y. Altintas, Modeling approaches and software for predicting the performance of milling operations at MAL-UBC, Mach. Sci. Technol. 4 (3) (2000) 445–478, https://doi.org/10.1080/10940340008945718.Publisher: Taylor & Francis

[4] Y. Altintas, A. Ber, Manufacturing automation: metal cutting mechanics, machine tool vibrations, and CNC design, Appl. Mech. Rev. 54 (5) (2001) B84, https://doi.org/10.1115/1.1399383.

[5] H.-Y. Feng, C.-H. Menq, The prediction of cutting forces in the ball-end milling process–I. Model formulation and model building procedure, Int. J. Mach. Tools Manuf. 34 (5) (1994) 697–710, https://doi.org/10.1016/0890-6955(94)90052-3.

[6] M. Fontaine, A. Devillez, A. Moufki, D. Dudzinski, Predictive force model for ball-end milling and experimental validation with a wavelike form machining test, Int. J. Mach. Tools Manuf. 46 (3) (2006) 367–380, https://doi.org/10.1016/j.ijmachtools.2005.05.011.

[7] C.-L. Tsai, Analysis and prediction of cutting forces in end milling by means of a geometrical model, Int. J. Adv. Manuf. Technol. 31 (9) (2007) 888–896, https://doi.org/10.1007/s00170-005-0275-7.

[8] H.U. Lee, D.-W. Cho, K.F. Ehmann, A mechanistic model of cutting forces in micro-end-milling with cutting-condition-independent cutting force coefficients, J. Manuf. Sci. Eng. 130 (3) (2008), https://doi.org/10.1115/1.2917300.

[9] S. Chinchanikar, S.K. Choudhury, Effect of work material hardness and cutting parameters on performance of coated carbide tool when turning hardened steel: an optimization approach, Measurement 46 (4) (2013) 1572–1584, https://doi.org/10.1016/j.measurement.2012.11.032.

[10] M.Y. Friedman, E. Lenz, The effect of thermal conductivity of tool material on cutting forces and crater wear rate, Wear 25 (1) (1973) 39–44, https://doi.org/10.1016/0043-1648(73)90118-X.

[11] M. Sekulić, Z. Jurković, M. Hadžistević, M. Gostimirović, The influence of mechanical properties of workpiece material on the main cutting force in face milling, Metalurgija 49 (4) (2010) 339–342.Publisher: Hrvatsko Metalursko Društvo (HMD)

[12] O. Cahuc, P. Darnis, R. Laheurte, Mechanical and thermal experiments in cutting process for new behaviour law, Int. J. Forming Processes 10 (2) (2007) 235–269, https://doi.org/10.3166/ijfp.10.235-269.

[13] O. Cahuc, P. Darnis, A. Gérard, J.-L. Battaglia, Experimental and analytical balance sheet in turning applications, Int. J. Adv. Manuf. Technol. 18 (9) (2001) 648–656, https://doi.org/10.1007/s001700170025.

[14] E. Olteanu, C. Bisu, I. Tănase, Determination of power consumption in milling, UPB Sci. Bull. Ser. D Mech. Eng. 75 (2013) 211–220.

[15] G. Albert, R. Laheurte, J.-Y. K'Nevez, P. Darnis, O. Cahuc, Experimental milling moment model in orthogonal cutting condition: to an accurate energy balance, Int. J. Adv. Manuf. Technol. 55 (9) (2011) 843–854, https://doi.org/10.1007/s00170-010-3118-0.

[16] O. Cahuc, C. Bisu, A. Gerard, Link between chips and cutting moments evolution, Adv. Mat. Res. 423 (2012) 89–102.Conference Name: Innovating Processes ISBN: 9783037853290 Publisher: Trans Tech Publications Ltd

[17] M.E. Martelloti, An analysis of the milling process, Trans. A.S.M.E. 63 (8) (1941) 677–700.

[18] O. Kienzle, Die bestimmung von kräften und leistungen an spanenden werkzeugen und werkzeugmaschinen, VDI-Z 94 (11) (1952) 299–305.

[19] R. Laheurte, O. Cahuc, P. Darnis, A. Gerard, Behaviour law for cutting process, Int. J. Adv. Manuf. Technol. 29 (1) (2006) 17–23, https://doi.org/10.1007/s00170-004-2498-4.

[20] R. Royer, O. Cahuc, A. Gerard, Strain gradient plasticity applied to material cutting, Adv. Mat. Res. 423 (2012) 103–115.Conference Name: Innovating Processes ISBN: 9783037853290 Publisher: Trans Tech Publications Ltd

[21] W. Yousfi, O. Cahuc, R. Laheurte, P. Darnis, M. Calamaz, 3D modelling of the mechanical actions of cutting: application to milling, in: B. Eynard, V. Nigrelli, S. M. Oliveri, G. Peris-Fajarnes, S. Rizzuti (Eds.), Advances on Mechanics, Design Engineering and Manufacturing : Proceedings of the International Joint Conference on Mechanics, Design Engineering & Advanced Manufacturing (JCM 2016), 14–16 September, 2016, Catania, Italy, Lecture Notes in Mechanical Engineering, Springer International Publishing, Cham, 2017, pp. 647–654, https://doi.org/10.1007/978-3-319-45781-9_65.

[22] W. Yousfi, O. Cahuc, R. Laheurte, P. Darnis, M. Calamaz, 3D milling modeling: mechanical actions, strains, strain rates and temperature calculations in the three cutting zones, Int. J. Adv. Manuf. Technol. 95 (5) (2018) 1931–1940, https://doi.org/10.1007/s00170-017-1351-5.

[23] M. San-Juan, O. Martín, F. Santos, Experimental study of friction from cutting forces in orthogonal milling, Int. J. Mach. Tools Manuf 50 (7) (2010) 591–600, https://doi.org/10.1016/j.ijmachtools.2010.03.013.

[24] G. Albert. Identification et modélisation du torseur des actions de coupe en fraisage, Bordeaux 1, 2010. These de doctorat.https://www.theses.fr/2010BOR14152